Noncontact Vital Sign Detection based on Stepwise Atomic Norm Minimization

Article · December 2015

1 author:

Hong Hong
Nanjing University of Science and Technology
23 PUBLICATIONS **72** CITATIONS

SEE PROFILE

Noncontact Vital Sign Detection based on Stepwise Atomic Norm Minimization

Li Sun, Hong Hong, *Member, IEEE*, Yusheng Li, Chen Gu, Feng Xi, *Member, IEEE*, Changzhi Li, *Senior Member, IEEE*, and Xiaohua Zhu, *Member, IEEE*

***Abstract*—Noncontact techniques for detecting vital signs have attracted great interest due to the benefits shown in medical monitoring and military applications. A rapid remote evaluation on physiological signal frequencies is needed in search and rescue operations as well as intensive care. However, the presence of respiration harmonics causes aliasing problems to heart-rate estimation, especially when the data volume is limited. By taking advantage of the simple pattern of physiological signals, we propose a stepwise atomic norm minimization method (StANM) to accurately assess the respiration and heartbeat frequencies with a limited data volume. First, the respiration frequency is estimated by the conventional atomic norm minimization. Then the frequencies of respiration harmonics are generated based on the inherent relationship between the fundamental tone and the harmonics. Finally, with the pre-estimated frequencies, we locate the heartbeat frequency by solving a modified atomic norm minimization problem. Simulations and experiments show that the proposed method can accurately estimate physiological frequencies from 6.5-second-long raw data with a 4-Hz sampling rate.**

***Index Terms*—Atomic norm minimization, line spectral estimation, noncontact, super-resolution, vital sign detection.**

I. Introduction

In RECENT years, noncontact vital sign detection technology has attracted great interest in various fields, such as medical monitoring, military applications, security and counter-terrorism action as well as search and rescue operations [1], [2]. It not only significantly extends the time that human subjects can be monitored, but also enables investigations on special problems such as empyrosis, and avoids the negative impact to measurement accuracy due to psychological factors. In some special medical applications such as intensive care, postoperative recovery of patients and monitoring of patients with severe trauma, a quick assessment of vital signs is of great importance for doctors to provide care. Also, prompt noncontact vital sign detection is crucial for quick evaluation of the status of soldiers on battlefield and search and rescue of trapped victims after earthquakes and fire disasters.

Existing baseband signal processing algorithms for noncontact vital sign detection are mainly based on the discrete Fourier transform (DFT). However, due to the smearing and leakage problems caused by limited data volume, the use of DFT suffers from significant performance degradation. In the previous attempts to improve the performance, Li *et al.* tried to adopt a parametric and cyclic optimization algorithm, namely, RELAX [3]. Simulation results showed that, for a 12.015-second-long data sampled at 20 Hz, this algorithm can separate the heartbeat component from the third-order harmonic of respiration with a frequency separation of 3 bpm. In 2013, the multiple signal classification (MUSIC) algorithm was applied to this field [4]. Experiments have demonstrated its feasibility in accurately estimating the heartbeat frequency during 8-28 s time intervals with a sampling rate of 100 Hz. Although via the RELAX and the MUSIC, the smearing and leakage problems can be alleviated to some extent, the required data volume is still quite large, which restricts their applications in short-time processing.

In an attempt to accurately assess respiration and heartbeat frequencies with a limited data length and a low sampling rate, we propose a novel method based on a stepwise version of the recently proposed atomic norm minimization (ANM) approach, which is proved to have a super-resolution capability with time-limited measurements [5]–[9]. In the next section, we will describe in detail how the aliasing problems are caused and what the harmful effects are. Then, the proposed method, namely, stepwise atomic norm minimization (StANM) will be elaborated in Section III, after a brief introduction on conventional ANM. Simulations and experiments are presented in Section IV to show the super-resolution capability of the StANM with a limited data volume. A conclusion will be provided in Section V.

II. Problem Description

Noncontact CW Doppler radars detect vital signs based on phase estimation of the signal reflected by a target [1]. The phase shift is generated by the time-varying displacement $x(t)$ of the target, which can be expressed as

$$x(t) = x_h(t) + x_r(t) \approx \alpha_h \sin(2\pi f_h t) + \alpha_r \sin(2\pi f_r t), \tag{1}$$

where $x_h(t)$ and $x_r(t)$ represent the heartbeat and respiration movements which can be approximated as sinusoidals with am-

Manuscript received July 01, 2015; revised September 25, 2015; accepted October 21, 2015. Date of publication October 26, 2015; date of current version October 30, 2015. This work was supported by the Special Foundation of China Postdoctoral Science under Grant 2013T6054, the National Natural Science Foundation of China under Grant 61301022, the Clinical Special Science Foundation of Science and Technology Department of Jiangsu Province under Grant BL2012062, and by the the Natural Science Foundation of Jiangsu Province under Grant SBK2014043201. The associate editor coordinating the review of this manuscript and approving it for publication was Prof. Mehdi Moradi.

L. Sun, H. Hong, Y. Li, C. Gu, F. Xi, and X. Zhu are with the School of Electronic and Optical Engineering, Nanjing University of Science and Technology, Nanjing 210094, China (e-mail: isunly@gmail.com; hongnju@njust.edu.cn).

C. Li is with the Department of Electrical and Computer Engineering, Texas Tech University, Lubbock, TX 79409 USA (e-mail: changzhi.li@ttu.edu).

Color versions of one or more of the figures in this paper are available online at http://ieeexplore.ieee.org.

Digital Object Identifier 10.1109/LSP.2015.2494604

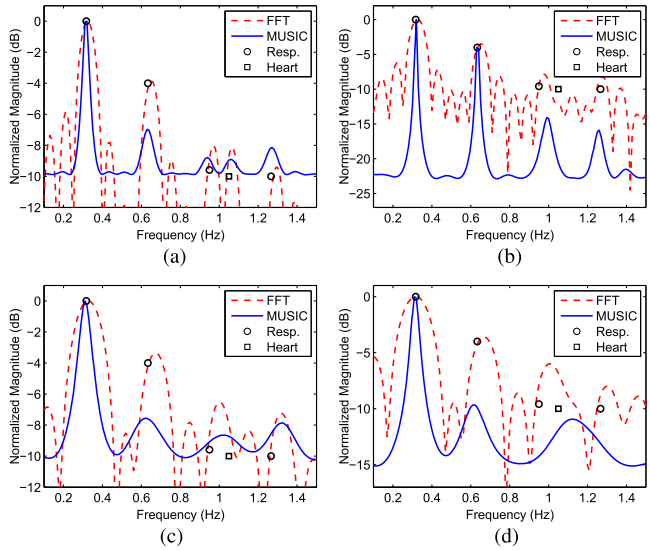

Fig. 1. Spectra given by FFT and MUSIC with different sampling rates and window lengths. The ground truth of heartbeat component is denoted by square, and those of respiration and its harmonics are denoted by circles. (a) $f_s = 100$ Hz, $T_0 = 13$ s (b) $f_s = 20$ Hz, $T_0 = 13$ s (c) $f_s = 100$ Hz, $T_0 = 6.5$ s (d) $f_s = 20$ Hz, $T_0 = 6.5$ s.

plitudes α_h and α_r and frequencies f_h and f_r, respectively. Using a complex signal demodulation, the received signal have the following form [3]

$$r(t) = \sum_{p=-\infty}^{\infty} \sum_{q=-\infty}^{\infty} C_{p,q} e^{j\theta} \cdot e^{j2\pi f_{p,q} t}, \tag{2}$$

where $C_{p,q} = J_p(4\pi\alpha_r/\lambda) \cdot J_q(4\pi\alpha_h/\lambda)$ represents the real-valued amplitude corresponding to the sinusoidal component with frequency $f_{p,q} = pf_r + qf_h$, and J_p is the pth-order Bessel function of the first kind [3]. Additionally, θ denotes the total phase residual accumulated along the transmission path and λ represents the wavelength.

Obviously, the above demodulation inevitably produces harmonics, which will severely affect the identification of heartbeat frequency because the 3rd- and 4th- order harmonics of respiration signal will have frequencies close to the heartbeat frequency. In order to illustrate this issue, a comparison of the spectra obtained by FFT with zero-padding and the MUSIC algorithm with different values of processing window length T_0 and sampling rate f_s is plotted in Fig. 1.

It is shown that both algorithms can separate the heartbeat and the harmonics of respiration with sufficient time-domain samples ($f_s = 100$ Hz and $T_0 = 13$ s), and the MUSIC provides a more accurate estimation. However, when the data volume is limited, neither algorithms can extract the heartbeat frequency, especially in the case with the most limited number of data ($f_s = 20$ Hz and $T_0 = 6.5$ s). Therefore, these limitations necessitate a reliable and accurate signal processing algorithm that can achieve high-resolution spectral estimation with a limited number of time-domain samples.

III. Stepwise Atomic Norm Minimization

Assuming that only K strongest sinusoids within a limited bandwidth are taken into consideration in Eq. (2), $r(t)$ can be modeled as a positive linear superposition of K line spectral atoms from an infinite set covering a continuous frequency band. It has been demonstrated that if the unknown frequencies of such sparse line spectral signal have sufficient separation, the ANM serves as the optimal predominant methodology to accurately estimate them with very limited number of data (sampled at a low rate and lasting for a short time) [6], [7]. However, this approach cannot be directly used to extract physiological frequencies, because the condition of "sufficient separation" is not always satisfied in practice, especially when the minimum frequency separation between heartbeat and respiration harmonics is small.

In order to resolve this inherent limitation, the StANM algorithm is proposed. The main concept of the StANM is to utilize a preliminary estimation on respiration frequency to generate the harmonic frequencies, and then locate the heartbeat frequency by solving a modified ANM problem with the estimated frequencies. The proposed algorithm is summarized as follows:

Step 1: **(ANM):** Recover the time sequence $\boldsymbol{r} \in \mathbb{C}^{N\times 1}$ from the noisy measurement $\boldsymbol{y} \in \mathbb{C}^{N\times 1}$ via the following semidefinite program

$$\begin{aligned} \underset{\boldsymbol{r},\boldsymbol{T},t}{\text{minimize}} \quad & \frac{\mu}{2N}\text{tr}(\boldsymbol{T}) + \frac{\mu}{2}t + \frac{1}{2}\|\boldsymbol{y}-\boldsymbol{r}\| \\ \text{subject to} \quad & \begin{bmatrix} \boldsymbol{T} & \boldsymbol{r} \\ \boldsymbol{r}^* & t \end{bmatrix} \succeq 0, \end{aligned} \tag{3}$$

where $\boldsymbol{T}$ is a Toeplitz matrix, $\text{tr}(\cdot)$ and $(\cdot)^*$ stand for the trace and the conjugate transpose of a matrix, respectively. N is the total data volume. Then the dual optimal solution $\boldsymbol{v}$ can be obtained by solving the dual problem

$$\begin{aligned} \underset{\boldsymbol{v},\boldsymbol{Q}}{\text{maximize}} \quad & \text{Re}(\boldsymbol{v}^*\hat{\boldsymbol{r}}) \\ \text{subject to} \quad & \begin{bmatrix} \boldsymbol{Q} & -\boldsymbol{v} \\ -\boldsymbol{v}^* & 1 \end{bmatrix} \succeq 0 \\ & \sum_{i=1}^{N-j} \boldsymbol{Q}_{i,i+j} = \begin{cases} 1, & j = 0 \\ 0, & j \in [1, N-1] \end{cases} \\ & \boldsymbol{Q} \text{is Hermitian.} \end{aligned} \tag{4}$$

After that, the physiological frequencies can be identified by verifying the dual polynomial

$$\left| \sum_{n=0}^{N-1} \hat{\boldsymbol{v}} e^{-j2\pi nf} \right| = \mu, \tag{5}$$

where its amplitude attains μ, which can be determined by a rough evaluation of the noise level. Finally, the corresponding amplitudes of these frequencies can be debiased by solving a least squares problem [6]. Note that this step also demonstrates a conventional ANM procedure, and can be solved efficiently via the alternating direction method of multipliers (ADMM) algorithm [10].

Step 2: Set the frequency with the maximum amplitude as the estimated respiration frequency $\hat{f}_1$. Then, based on the inherent relationship with $\hat{f}_1$, we generate the harmonic frequencies $\hat{f}_k = k\hat{f}_1$, $k = 2, 3, \ldots, K-1$, some of which might be very close to the heartbeat frequency.

Step 3: Solve a modified semidefinite program as below

$$\begin{aligned} \underset{\boldsymbol{r},\boldsymbol{r}_{\rm res},\boldsymbol{T},t,\beta_k}{\text{minimize}} \quad & \frac{\mu}{2N}\text{tr}(\boldsymbol{T}) + \frac{\mu}{2}t + \frac{1}{2}\|\boldsymbol{y}-\boldsymbol{r}\| \\ \text{subject to} \quad & \begin{bmatrix} \boldsymbol{T} & \boldsymbol{r}_{\rm res} \\ \boldsymbol{r}_{\rm res}^* & t \end{bmatrix} \succeq 0 \\ & \boldsymbol{r} = \boldsymbol{r}_{\rm res} + \sum_k \beta_k \boldsymbol{a}_k, k \in \mathcal{P}, \end{aligned} \tag{6}$$

where $\mathcal{P}$ is the set of indices for the pre-estimated frequencies $\hat{f}_k$, β_k is the amplitude to be estimated, and $\boldsymbol{a}_k = [1 \quad e^{j2\pi\hat{f}_k} \quad \dots \quad e^{j2\pi(N-1)\hat{f}_k}]^{\rm T}$ is the atom of the kth frequency. Similar to Step 1, the dual optimal solution $\hat{\boldsymbol{v}}_{\rm res}$ is calculated with the residual optimal $\hat{\boldsymbol{r}}_{\rm res}$, and the heartbeat frequency is determined by finding the one with dominant debiased amplitude.

Based on precise estimation of respiration frequency, the generated harmonics are well suppressed during the subsequent minimization. So the residual part $\boldsymbol{r}_{\rm res}$ will very likely be dominated by the heartbeat, which alleviates the performance degradation caused by an insufficient frequency separation, thus enhancing the robustness of heart-rate estimations.

Note that once a respiratory harmonic frequency is located near the heartbeat frequency, their spectra may merge into a single spike. In this situation, our method may not distinguish them. The solution is to go back to the result of step 1, and just identify the component with the maximum peak value in a reasonable heart-rate range (e.g., [0.8, 2] Hz) as the heartbeat frequency, since the corresponding bias would be very small (probably smaller than a tolerable error).

IV. Simulations and Experiments

A. Performance Evaluation

To verify the superiority of the StANM, a similar instance as in Section II was simulated. According to the harmonic model in Eq. (2), the simulated respiration and heartbeat signals were set as 19 bpm (0.317 Hz) and 65 bpm (1.083 Hz), respectively, and the second- to forth-order harmonics of respiration were included, with amplitudes satisfying $|\beta_r| : |\beta_{r_2}| : |\beta_{r_3}| : |\beta_{r_4}| : |\beta_h| = 10 : 4 : 1.2 : 1 : 1$ [3]. The processing window was set as 6.5 s, and the data was sampled at 100 Hz for the FFT and the MUSIC. On the other hand, only 4 Hz sampled sequence was provided for the ANM and the StANM, which leads to a very limited data volume of $N = 26$ samples. A reflected signal lasting for 60 s was generated, and an additive Gaussian noise was added so that SNR $= 20$ dB in order to approximate practical laboratory environments. The observed spectral scope was from 0.1 Hz to 2 Hz. To achieve robust results via the MUSIC, the signal and noise subspace were divided by setting $P = 64$ according to [4].

In Fig. 2, a comparison for FFT, MUSIC, ANM and StANM algorithms is presented, with a randomly chosen data frame. Obviously, all of the four algorithms can give accurate estimations of respiration frequencies. However, except for the StANM, none of these methods can distinguish the heartbeat frequency from the 3rd harmonic of respiration. The FFT gives a fuzzy spectrum full of sidelobes, while the MUSIC mixes the heartbeat component with the harmonics. Similar problem is found in conventional ANM: because the minimum separation condition

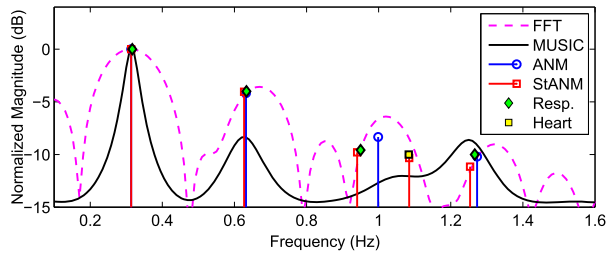

Fig. 2. Spectra estimated by FFT, MUSIC, ANM and StANM algorithms using a randomly chosen 6.5-s data frame. The ground truth of heartbeat component is denoted by square, and those of respiration and its harmonics are denoted by diamonds.

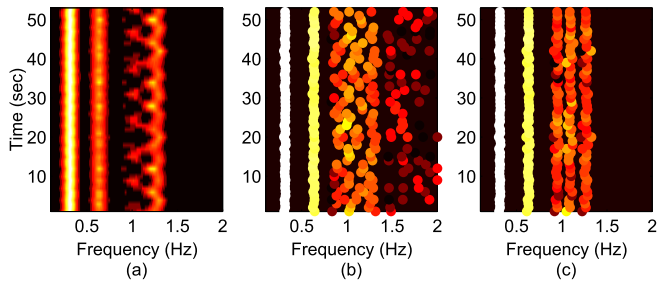

Fig. 3. Time-varying results given by (a) MUSIC, (b) ANM and (c) StANM respectively. The processing window is set as 6.5 s, and the interval of two successive frames is 1 s. The simulated respiration and heartbeat rates are set as 19 bpm (0.317 Hz) and 65 bpm (1.083 Hz), respectively.

is no longer satisfied due to the very short processing window length, only a frequency of 0.998 Hz is identified. Benefitting from the accurate pre-estimation, the harmonic interferences are suppressed when solving the modified ANM in Step 3. Therefore, by using the StANM, the heartbeat frequency is successfully identified as 1.085 Hz.

To further compare the ability in extracting the heartbeat component, the time-varying results of MUSIC, ANM and StANM are plotted in Fig. 3. All these algorithms can give robust frequency estimation on strong respiration, but only the proposed method is able to reliably track the heartbeat frequency. Although the MUSIC generates one track within the concerned heartbeat frequency range, this frequency is biased to the 4th-order harmonic (1.27 Hz). Conventional ANM tends to distinguish the heartbeat from the 3rd and 4th harmonics in some frames, but still cannot give a robust result. On the contrary, an accurate track of 1.09 Hz is obtained using the StANM.

In Fig. 4, a comparison on the accuracy of heartbeat estimation is conducted by calculating root-mean-square error (RMSE) with data length varying from 5.12 s to 14.4 s. The simulation settings are the same as those in Fig. 3. Obviously, with a lower sampling rate of 20 Hz, the MUSIC fails across the evaluation scope. When the sampling rate increases to 100 Hz, the RMSEs can be improved to an acceptable level when the data length exceeds 11 s. These results coincide with the problem raised in Section II. While for conventional ANM, a much lower sampling rate of 4 Hz is enough to achieve smaller RMSEs than the MUSIC (100 Hz) when data length exceeds 8 s. But it still fails with extreme short data length. Benefiting from the stepwise process, the StANM can work with both a low sampling rate (4 Hz) and a short data length (6.5 s), and is able to obtain smaller RMSEs across the evaluation scope. Meanwhile, due to the use of ADMM, the computation time of

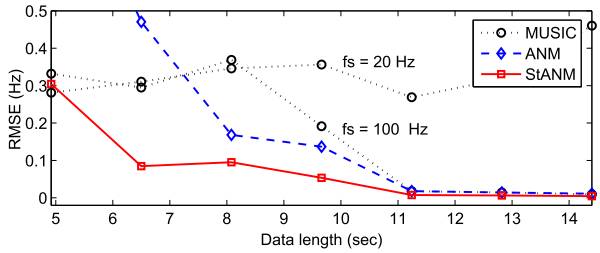

Fig. 4. Comparison of the accuracy of heartbeat estimation for different data lengths. The simulated respiration and heartbeat rates are set as 19 bpm (0.317 Hz) and 65 bpm (1.083 Hz), respectively. SNR $= 20$ dB. The sampling rate of the ANM-based algorithms is 4 Hz.

Fig. 5. The applied CW Doppler radar system with five building blocks: (I) Two 2.4 GHz microchip patch antenna arrays and radar receiver. (II) 2.475 GHz local oscillator. (III) The ADC and FPGA quadrature down-converter. (IV) Desktop for subsequent signal processing. (V) The traditional vital sign monitor (JP2000-09).

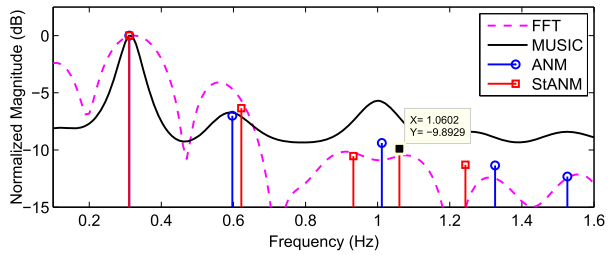

Fig. 6. Spectra estimated by FFT, MUSIC, ANM and StANM algorithms using a randomly chosen 6.5-s data frame. The references of respiration and heartbeat rate obtained by JP2000-09 are 19 bpm (0.317 Hz) and 66 bpm (1.1 Hz), respectively.

TABLE I
SUCCESSFUL ESTIMATION RATES WITH EXPERIMENTAL DATA

		MUSIC		StANM	
Subject	Distance	Respiration	Heartbeat	Respiration	Heartbeat
A	1 m	97.3 %	58.7 %	100 %	90.7 %
	2 m	94.7 %	70.7 %	100 %	93.3 %
	3 m	96 %	64 %	100 %	86.7 %
B	1 m	100 %	62.5 %	100 %	89.3 %
	2 m	94.6 %	66.1 %	100 %	96.4 %
	3 m	91.1 %	58.9 %	98.2 %	92.9 %
C	1 m	96 %	69.3 %	100 %	92 %
	2 m	98.7 %	76 %	100 %	94.7 %
	3 m	93.3 %	65.3 %	100 %	88 %

the ANM-based algorithms is in the same order of magnitude as the MUSIC (10^{-1} s) with 6.5-second-long data. But as the data length grows to be larger than 11 s so that the MUSIC becomes applicable, the computation time of MUSIC increases to the order of 10^{0} s, while that of the ANM-based algorithms remains to be the order of 10^{-1} s. This shows the potential of our algorithm in real-time processing.

B. Experimental Validation

For laboratory experiments, a CW Doppler radar similar to our previous work [11], [12] was designed. The configuration is illustrated in Fig. 5. The carrier frequency was chosen to be 2.475 GHz and the transmit power was set as -13 dBm. A 75 MHz intermediate frequency signal was digitized and down-converted for subsequent signal processing. A traditional vital sign monitor (JP2000-09) was used as a reference.

Fig. 6 demonstrates a comparison of spectral estimation with the data acquired by this system. The parameters for signal processing are the same as the simulations presented in Section IV-A, and a 6.5-second-long data frame was randomly chosen. The subject was seated 2 meters away from the antenna. The experimental results coincide with that shown in Fig. 2, where all these algorithms perform well in estimating respiration frequency, but only the StANM succeed in distinguishing the heartbeat component from the harmonics. The heart rate estimated via StANM is 64 bpm (1.06 Hz), which is close to the 66 bpm (1.1 Hz) measured by JP2000-09.

More experiments were conducted with three young heathy males (A: 171 cm, 63 kg, B: 182 cm, 74 kg, and C: 174 cm, 69 kg) from three different distances to show the robustness of our proposed algorithm. In each experiment, a real-time processing lasting for at least 80.94 s was carried out. The frame length was set as 6.5 s, and the interval between two successive frames was 1 s. The time-varying results were evaluated by calculating the bias $E = |\hat{f} - f_0|/f_0$ in each frame, and counting the frames when $E < 5\%$. $\hat{f}$ and f_0 represent the frequencies obtained via our noncontact system and JP2000-09, respectively. The details are shown in Table I. It is easy to conclude that both algorithms can give robust estimation of respiration frequencies at every distance, with the successful rates of the StANM being slightly higher. However, the successful rates of heartbeat frequency estimation of the MUSIC stay around 65%, which are much lower than those given by the StANM (around 90%). The results have validated the robustness of our algorithm.

V. CONCLUSION

In conclusion, a novel approach for noncontact vital sign detection based on atomic norm minimization is presented. By exploiting the multiple relationships between respiration and its harmonics, a stepwise procedure is proposed to enhance heartbeat frequency identification. Simulations and experiments showed that the proposed method can effectively distinguish heartbeat component from closely located respiration harmonics in frequency domain with very limited data volume (4 Hz sampling rate, 6.5 s duration). This leads to a significant advantage for the proposed method to be used in health care and medical research applications.

REFERENCES

[1] C. Li, V. M. Lubecke, O. Boric-Lubecke, and J. Lin, "A review on recent advances in doppler radar sensors for noncontact healthcare monitoring," *IEEE Trans. Microwave Theory Techn.*, vol. 61, no. 5, pp. 2046–2060, 2013.

[2] E. Conte, A. Filippi, and S. Tomasin, "Ml period estimation with application to vital sign monitoring," *IEEE Signal Process. Lett.*, vol. 17, no. 11, pp. 905–908, 2010.

[3] C. Li, J. Ling, J. Li, and J. Lin, "Accurate doppler radar noncontact vital sign detection using the RELAX algorithm," *IEEE Trans. Instrum. Meas.*, vol. 59, no. 3, pp. 687–695, 2010.

[4] P. Bechet, R. Mitran, and M. Munteanu, "A non-contact method based on multiple signal classification algorithm to reduce the measurement time for accurately heart rate detection," *Rev. Sci. Instrum.*, vol. 84, no. 8, p. 084707, 2013.

[5] E. J. Candès and C. Fernandez-Granda, "Towards a mathematical theory of super-resolution," *Commun. Pure Appl. Math.*, vol. 67, no. 6, pp. 906–956, 2014.

[6] B. N. Bhaskar, G. Tang, and B. Recht, "Atomic norm denoising with applications to line spectral estimation," *IEEE Trans. Signal Process.*, vol. 61, no. 23, pp. 5987–5999, 2013.

[7] G. Tang, B. N. Bhaskar, P. Shah, and B. Recht, "Compressed sensing off the grid," *IEEE Trans. Inf. Theory*, vol. 59, no. 11, pp. 7465–7490, 2013.

[8] Z. Yang and L. Xie, "On gridless sparse methods for line spectral estimation from complete and incomplete data," *IEEE Trans. Signal Process.*, vol. 63, no. 12, pp. 3139–3153, 2015.

[9] Y. Chi and Y. Chen, "Compressive two-dimensional harmonic retrieval via atomic norm minimization," *IEEE Trans. Signal Process.*, vol. 63, no. 4, pp. 1030–1042, 2015.

[10] D. P. Bertsekas and J. N. Tsitsiklis*, Parallel and Distributed Computation: Numerical Methods*. Upper Saddle River, NJ, USA: Prentice-Hall, 1989.

[11] L. Sun, Y. Li, H. Hong, F. Xi, W. Cai, and X. Zhu, "Super-resolution spectral estimation in short-time non-contact vital sign measurement," *Rev. Sci. Instrum.*, vol. 86, no. 4, p. 044708, 2015.

[12] H. Zhao, H. Hong, L. Sun, F. Xi, C. Li, and X. Zhu, "Accurate dc offset calibration of doppler radar via non-convex optimisation," *Electron. Lett.*, vol. 51, no. 16, pp. 1282–1284, 2015.